

## Geochronology of sediments in the Cananeia-Iguape estuary and in southern continental shelf of São Paulo State, Brazil

R. T. Saito,<sup>1</sup> R. C. L. Figueira,<sup>1</sup> M. G. Tessler,<sup>2</sup> I. I. L. Cunha<sup>1,\*</sup>

<sup>1</sup> IPEN/CNEN-SP (TFR)

<sup>2</sup> Oceanographic Institute, University of São Paulo, 05422-970 – Pinheiros, São Paulo, Brazil

(Received December 11, 2000)

Instrumental analysis methods for <sup>210</sup>Pb, <sup>226</sup>Ra and <sup>137</sup>Cs by gamma-spectrometry in sediments, as well as the sedimentation rates in cores collected from Brazilian coastal region are presented. Sampling locations have covered the Cananeia-Iguape estuary and the continental shelf of southern Sao Paulo State. Values for <sup>210</sup>Pb ranged from 122.5 to 14.3 Bq·kg<sup>-1</sup> for estuarine sediments and from 195.5 to 23.6 Bq·kg<sup>-1</sup> at the continental shelf. For <sup>226</sup>Ra the values obtained in sediments varied from 15.2 to 2.3 Bq·kg<sup>-1</sup> in the estuary and from 30.1 to 16.1 Bq·kg<sup>-1</sup> at the continental shelf. Sedimentation rates are variable, ranging from 0.53 to 0.98 cm·y<sup>-1</sup> in estuary sediments and from 0.18 to 0.40 cm·y<sup>-1</sup> at the continental shelf.

### Introduction

Coastal systems, in particular the estuaries, are the first depositional environment to receive sediments transported from rivers to the oceans. As a consequence of the geochemical process, sediments present in the estuary may be submitted to a series of transformations. Part of the sediment can be deposited in the estuary and the remaining sediment may flow into the ocean, being transported and deposited under influence of tides and maritime currents.

In the last decades, the intensive human activity along the estuarine regions has significantly increased the sediment inflow in these locals and consequently, the sediment accumulation in the estuarine channels and in the ocean. The use of <sup>210</sup>Pb to date sediments up to 100 years is a very important tool to establish a geochronology of the coastal environment.<sup>1–4</sup> Other radionuclides, such as <sup>137</sup>Cs, are often used to determine sedimentation rates in addition to those provided by <sup>210</sup>Pb measurements. So, distributions of <sup>210</sup>Pb and <sup>137</sup>Cs within the sediment sequence may provide more precise data for calculating sedimentation rates in coastal environment.<sup>5–8</sup>

The purpose of this work was to establish instrumental analysis methods for <sup>210</sup>Pb, <sup>226</sup>Ra and <sup>137</sup>Cs in sediments by gamma-spectrometry and to determine levels of these radionuclides in sediment cores collected from the Cananeia-Iguape estuary and from the southern continental shelf of Sao Paulo State. Sedimentation rates have been evaluated from the excess <sup>210</sup>Pb and <sup>137</sup>Cs profiles at these locations in order to elucidate the sedimentation process.

### Cananeia – Iguape estuary

Comprida Island, a barrier island, separates the Cananeia-Iguape (25°S–48°W) from the ocean and is approximately 70 km long. The genesis of this coastal plain is directly connected to the variation of the sea level along the Superior Quarter. The area was partially covered with seawater reaching between 8 and 10 m, respectively, above the present level in the Pleistocene and between 4 and 5 m in the Holocene event.

In the interval between the transgressive maximums, with the pronounced retirement of the sea level exposing the present coastal plain totally, sand strings have been depositing on a set of transitional sand-clay sediments and transgressive seaside sands. In this regressive event, reaching a peak about 17,000 years BP, the exposed sediments were affected by erosion and gave origin to valleys which, during the following transgressive event, were covered with water; turning into large lagoons, where sand-clay sediments, rich in organic material, have deposited.

From the transgressive Holocene maximum, when the coastal line retired to its present level towards NE a long barrier island was formed (Comprida Island) by the action of seaside moving currents, causing the formation of the Cananeia-Iguape estuary, at the back of the present coastal line. In the NE of this coastal system the mouth of the Ribeira de Iguape river is located. The largest drainage system of the south-eastern Brazilian seashore, draining all the mountainous crystalline complex behind the coastal plain, communicates with Cananeia-Iguape estuary only through an artificial canal, built over 150 years ago.

\* E-mail: macunha@ipt.br

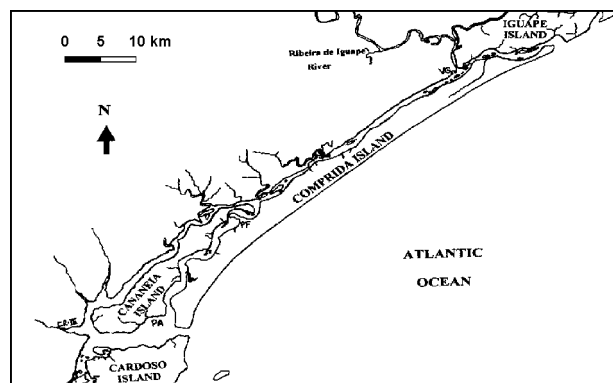


Fig. 1. The Cananeia-Iguape estuary

Today, about 60% of the Ribeira de Iguape river discharge flows in the internal canals of the Cananeia-Iguape estuary, causing an increasing silting up of the canals by the muddy sediments carried in suspension by the drainage of the Ribeira de Iguape. Thus, the continental material is transferred to the maritime system in the southern seashore of Sao Paulo State, not only in the mouth of the Ribeira de Iguape river but also in the river mouths of the Cananeia-Iguape estuary. This estuary is located 70 km southwest of the Ribeira de Iguape mouth. (Fig. 1).

#### *The continental shelf*

The continental shelf, in the studied area, presents a width ranging from 73 to 231 km, inclination between 1:656 and 1:1333 with a depth of transition between the platform and the continental slope located between 120 and 180 m depth.

During the geological evolution, a network of undersea canals and valleys was developed on the continental platform and slopes.

#### *Dynamics of water masses on the south-eastern/south continental coastal line of Brazil*

The dynamics of water masses on the south-eastern/south Brazilian continental coast is a process of interaction of three main water masses: coastal water (CW); tropical water (TW); and the South Atlantic central water (ACAS), which present strongly seasonal characteristics in their relocations on the continental shelf.<sup>9</sup>

This seasonal characteristic is observed with the penetration of the ACAS, a mass of cold and denser water, close to the sea bottom, from the deep ocean towards the coastal line. This penetration makes the shallow and less dense masses of waters to relocate in the surface to more external portions of the continental margin, keeping the TW relatively far from the coast.

As the summer also corresponds to the time of heavier rainfall on the Sao Paulo coast and, therefore,

increases the flow in the river systems, the dynamic process of superficial water relocation can represent a potential period of greater suspended terrestrial sediment and organic matter exportation to the ocean.<sup>10</sup>

By the end of summer, and more intensely during the winter, with the retirement of ACAS to the external platform and upper slope, the TW starts to have more influence on the continental shelf and the CW does not project into more external sections of the platform.

There seems to be a greater stability in the dynamics of the water masses in the more external sections of the continental shelf, the slope and deeper grounds. The TW has influence up to 200 m depth, followed by the ACAS, which goes as far as 600 m deep and interferes with the development of a pronounced thermocline. Below the ACAS relocate, in a northwards row, the Antarctic Intermediate Water (AIW), to about 2,500 m depth and southwards the Deep Water of the Antarctic Water (DAW), from 3,500 m to the bottom of the ocean bays.

## **Experimental**

### *Equipment*

Gamma-ray spectrometer, low background Ge detector, EG&G ORTEC, GEM 60120P Model, with a resolution of 1.9 keV at 1332.40 keV photopeak of <sup>60</sup>Co. The software of the data acquisition was MAESTRO II.<sup>11</sup>

Sediment cores were collected with a standard box core of 20×30 cm<sup>2</sup> cross sectional area at the continental shelf, or with a cylindrical PVC container of 50×7 cm in the estuary.

### *Sediment sampling*

Cores were collected by the Oceanographic Institute, University of Sao Paulo, Brazil, at three stations of the continental shelf and at three stations of the estuary (PA, PF and CR-III, that show different sediment inflow to the coastal system). Sand and mud contents (silt and clay) were analyzed in each core. The cores were sliced into 2 cm thick layers, dried and homogenized, and transferred to plastic containers appropriate for gamma-counting. The contents of organic matter and humidity were determined in every core.

### *Methodology for <sup>210</sup>Pb analysis*

<sup>210</sup>Pb was assayed by gamma-counting by means of its photopeak of 47 keV as described below. The method consisted of detector calibration, determination of detector counting efficiency, cumulative counting of both background and samples in regular intervals of counting time, photopeak smoothing and linear regression.

Detector calibration was performed by means of several gamma-ray emitting nuclides. IAEA reference materials were employed to determine the detector counting efficiency in the radionuclide photopeak region.

#### Background radiation

The environmental samples present a low activity, so any background radiation influences the detection of the radionuclide. A study of the background radiation variation in the region of  $^{210}\text{Pb}$  photopeak, as a function of time was performed.

Cumulative background counting was carried out for 150,000 seconds, in intervals of 10,000 seconds. The counting time to be employed depended on the  $^{210}\text{Pb}$  level in the sample, in order to improve counting statistics. A linear regression was fitted through data ranging from 70,000 to 150,000 seconds.

The gamma-spectrum was smoothed according to a binomial algorithm, which replaces the original data, channel by channel, with the smoothed data.

It was noticed that the ideal number of channels for the analysis was eleven and any variation in the channel versus energy function could lead to error in the analysis (change in the photopeak of  $^{210}\text{Pb}$ ). Therefore, the spectrum must be often re-calibrated to the channel position previously specified.<sup>12</sup>

#### Sample analysis

The same process carried out to obtain the accumulative background counting was repeated for the

sediment sample. Comparison between the linear regression curves of background and sediment sample allowed for the determination of sediment radionuclide activity, discounting background activity for each registered time.

$^{210}\text{Pb}$  activity was calculated according to the following equation:

$$(A_{\text{Pb-210}} \pm \sigma_{\text{Pb-210}}) = \frac{(C_s \pm \sigma_s) - (C_{\text{Bg}} \pm \sigma_{\text{Bg}})}{m_s \cdot t \cdot (\epsilon \pm \sigma_\epsilon)}$$

where  $A_{\text{Pb-210}}$  is the  $^{210}\text{Pb}$  activity in the sample,  $\text{Bq}\cdot\text{kg}^{-1}$ ;  $C_s$  is the  $^{210}\text{Pb}$  gross counting in the sample;  $C_{\text{Bg}}$  is the background counting;  $m_s$  is the sample mass, kg;  $t$  is the counting time, s;  $\epsilon$  is the counting efficiency for the  $^{210}\text{Pb}$  photopeak (47 keV);  $\sigma$  is the standard deviations of the variables.

Analyses of  $^{226}\text{Ra}$  and  $^{137}\text{Cs}$  were performed as above mentioned, by using the photopeak 609 and 661 keV, respectively. For  $^{226}\text{Ra}$  measurements, the packed samples were stored for 20 days in order to reach radioactive equilibrium. Excess  $^{210}\text{Pb}$  (unsupported) was calculated by subtracting the  $^{226}\text{Ra}$  ( $^{210}\text{Pb}$  supported) radioactivity from the  $^{210}\text{Pb}$  total radioactivity.

## Results and discussion

In order to verify if the methods developed here were adequate to the radionuclide analysis, they were applied to reference materials. Table 1 presents the results obtained in the analysis of reference samples.

Table 1.  $^{210}\text{Pb}$ ,  $^{226}\text{Ra}$  and  $^{137}\text{Cs}$  levels in reference materials

Reference material	$^{210}\text{Pb}$ , $\text{Bq}\cdot\text{kg}^{-1}$	$^{226}\text{Ra}$ , $\text{Bq}\cdot\text{kg}^{-1}$	$^{137}\text{Cs}$ , $\text{Bq}\cdot\text{kg}^{-1}$
SOIL-6 (Soil)			54 ± 1 53.65 (51.43–57.91)*
IAEA-300 (Marine Sediment)	343 ± 8 360 (339–395)*	51 ± 2 56.5**	
IAEA/307 (Sea plant)		3.0 ± 0.2 3.1 (2.1–4.4)*	4.7 ± 0.5 4.9 (4.5–5.2)*
IAEA-308 (Seaweed)	61 ± 1 73 (66–75)*		
IAEA/315 (Marine Sediment)		17.6 ± 0.3 14.2 (13.2–15.8)*	
IAEA-327 (Soil)	57 ± 3 52.70 (46.98–58.42)*		
IAEA-352 (Fish)			3.3 ± 0.5 2.7 (2.5–2.8)*
IAEA-368 (Marine Sediment)	26 ± 1 23.2 (19.8–27.2)*	26 ± 1 21.4 (20.3–22.6)*	
IAEA/SD-N-2 (Marine Sediment)			0.61 ± 0.09 0.8 (0.5–1.0)*

\* Certified values.<sup>13</sup>

\*\* Indicated values and confidence interval ( $\alpha = 0.05$ ).

Table 2. Results of the intercomparison analysis of the IAEA-384 sample

Radionuclide	Obtained value, Bq·kg <sup>-1</sup>	Certified value, <sup>13</sup> Bq·kg <sup>-1</sup>
<sup>210</sup> Pb	20.1 ± 0.7	20.4 (18.9–21.86)
<sup>137</sup> Cs	0.57 ± 0.03	0.31 (0.235–0.62)

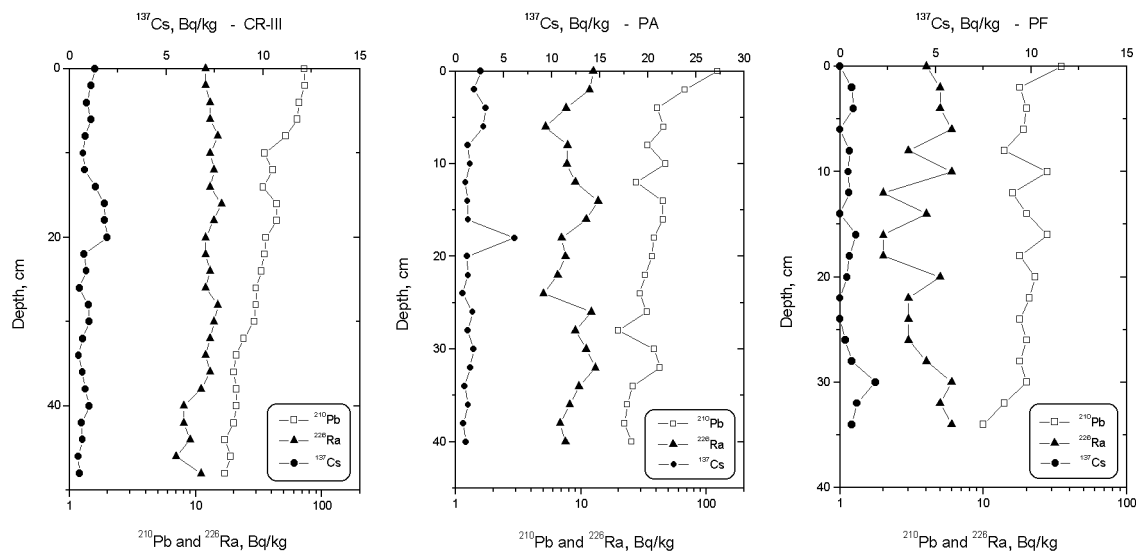


Fig. 2. Profiles of <sup>210</sup>Pb total, <sup>226</sup>Ra and <sup>137</sup>Cs levels in the cores of Cananéia-Iguape estuary

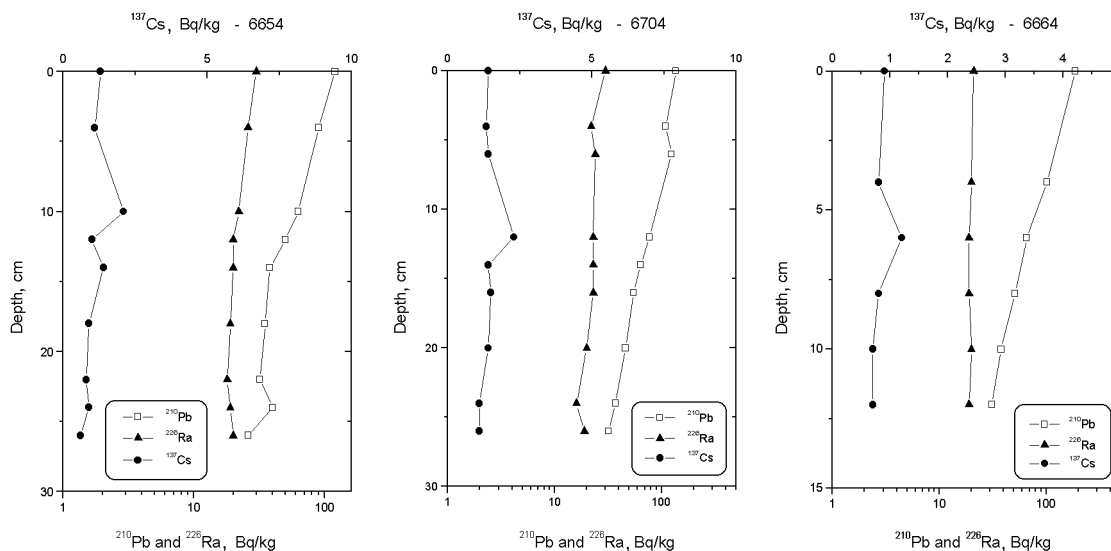


Fig. 3. Profiles of <sup>210</sup>Pb total, <sup>226</sup>Ra and <sup>137</sup>Cs in the cores of the continental shelf

The results in Table 1 show the analysis precision ranged from 2 to 5% for <sup>210</sup>Pb, from 2 to 7% for <sup>226</sup>Ra. By comparison with recommended values, reference samples that contain a <sup>137</sup>Cs level of about 0.8 Bq·kg<sup>-1</sup> show a relative error of 23%, but it decreases to 0.6% as

<sup>137</sup>Cs levels reaches 50 Bq·kg<sup>-1</sup>. The methods showed good precision and accuracy and the methodology is favourable to routine monitoring purposes, especially with small photopeaks.

We have also participated in a comparison analysis run by the International Atomic Energy Agency (IAEA). The results obtained for the analysis of IAEA-384 sample (Fangataufa sediment) are presented in Table 2 and it could be concluded that the values obtained by our laboratory are in good agreement with the certified values, indicating that the methods developed here can be applied to the analysis of the radionuclides  $^{210}\text{Pb}$  and  $^{137}\text{Cs}$ .

#### $^{210}\text{Pb}$ , $^{226}\text{Ra}$ and $^{137}\text{Cs}$ in sediment cores

Results obtained in the analysis of the radionuclides in sediment cores collected in the Cananeia-Iguape estuary and in the continental shelf, are given in Figs 2 and 3.

$^{210}\text{Pb}$  levels in the estuary varied from 122.5 to 14.3  $\text{Bq}\cdot\text{kg}^{-1}$  and for  $^{226}\text{Ra}$  ranged from 15.2 to 2.3  $\text{Bq}\cdot\text{kg}^{-1}$ . In the continental shelf the values varied from 195.5 to 23.6  $\text{Bq}\cdot\text{kg}^{-1}$  and from 30.1 to 16.1  $\text{Bq}\cdot\text{kg}^{-1}$ , respectively.  $^{210}\text{Pb}$  levels are much higher in the upper layers of the core and decreased with the depth.

These results are consistent with the values published in the literature. RAVICHANDRAN et al.<sup>3</sup> studied the geochronology of sediments in the Sabine-Neches estuary, Texas, USA and found  $^{210}\text{Pb}$  levels ranged from 87 to 30  $\text{Bq}\cdot\text{kg}^{-1}$  and for  $^{226}\text{Ra}$  from 67 to 25  $\text{Bq}\cdot\text{kg}^{-1}$ . The concentration of  $^{210}\text{Pb}$  and  $^{226}\text{Ra}$  in bottom sediments in Chesapeake Bay varied from 124.8 to 14.3  $\text{Bq}\cdot\text{kg}^{-1}$  and 29.8 to 4.3  $\text{Bq}\cdot\text{kg}^{-1}$ , respectively.<sup>14</sup> MCDONALD et al.<sup>15</sup> obtained  $^{210}\text{Pb}$  levels in sediments in Great Britain, ranging from 18.6 to 33.7  $\text{Bq}\cdot\text{kg}^{-1}$ .

The concentration of  $^{210}\text{Pb}$  and  $^{226}\text{Ra}$  in the continental shelf sediments from the East Chukchi Sea<sup>16</sup> ranged from 42.0 to 15.3  $\text{Bq}\cdot\text{kg}^{-1}$  and 22.5 to 13.7  $\text{Bq}\cdot\text{kg}^{-1}$ , respectively. In sediments from the eastern continental margin of the Arabian Sea<sup>8</sup> levels were obtained for  $^{210}\text{Pb}$  varying from 514 to 21  $\text{Bq}\cdot\text{kg}^{-1}$  and for  $^{226}\text{Ra}$  from 96.7 to 2.3  $\text{Bq}\cdot\text{kg}^{-1}$ .

$^{137}\text{Cs}$  levels obtained here in the Cananeia-Iguape estuary ranged from 0.28 to 6.1  $\text{Bq}\cdot\text{kg}^{-1}$  and at continental shelf the values ranged from 0.62 to 2.29  $\text{Bq}\cdot\text{kg}^{-1}$ . The presence of  $^{137}\text{Cs}$  in the Brazilian sediments is due to world-wide fallout. FIGUEIRA et al.<sup>17</sup> measured the  $^{137}\text{Cs}$  levels in the sediments of the southern continental shelf of Brazil. The levels varied from 1.0 to 1.8  $\text{Bq}\cdot\text{kg}^{-1}$ . Data published in the literature show different values depending on the presence of nuclear reprocessing plants or of the influence on the Chernobyl accident. In sediments at the Syria coast<sup>18</sup>  $^{137}\text{Cs}$  levels varied from 0.75 to 1.39  $\text{Bq}\cdot\text{kg}^{-1}$  while sediments collected in the San Francisco bay<sup>7</sup> presented levels ranging from 0.03 to 6.25  $\text{Bq}\cdot\text{kg}^{-1}$ .  $^{137}\text{Cs}$  concentration in sediment collected from the deep basins of the East Sea (Sea of Japan)<sup>19</sup> ranged from 8.3 to 25.4  $\text{Bq}\cdot\text{kg}^{-1}$ .

Table 3. Sedimentation rates in the Cananeia-Iguape estuary and in the southern continental shelf of São Paulo State

Core	Sedimentation rate of $^{210}\text{Pb}$ , $\text{cm}\cdot\text{y}^{-1}$	Sedimentation rate of $^{137}\text{Cs}$ , $\text{cm}\cdot\text{y}^{-1}$
PF	0.98	0.91
CR-III	0.62	0.61
PA	0.53	0.55
6704	0.40	0.29
6654	0.33	0.29
6664	0.18	0.15

#### Sedimentation rates

Table 3 and Fig. 4 show the sedimentation rates obtained in the Cananeia-Iguape estuary and in the continental shelf by using  $^{210}\text{Pb}$  and  $^{137}\text{Cs}$  dating.

By  $^{210}\text{Pb}$  dating, the estuarine sediments presented sedimentation rates varying from 0.53 to 0.98  $\text{cm}\cdot\text{y}^{-1}$ . At the continental shelf, the sedimentation rates varied from 0.18 to 0.4  $\text{cm}\cdot\text{y}^{-1}$ .  $^{137}\text{Cs}$  profiles showed distinct peaks corresponding to the maximum fallout in 1963–1964. By using these peaks the sedimentation rates were estimated.<sup>5,20,21</sup> The results are in good agreement with the measurements of  $^{210}\text{Pb}$  (exception of sample 6704). Some authors have showed the importance of the use of more than one radionuclide in the sedimentation rate studies in marine environment.<sup>5,8,20–22</sup>

#### Conclusions

The results obtained during the analyses of the reference materials and the intercomparison exercises were in agreement with the certified values for the three radionuclides, indicating that these methods can be applied to the analyses of radionuclides present in low concentration.

The levels of  $^{210}\text{Pb}$  in the cores PA, PF and CR-III show a fall with the depth and  $^{137}\text{Cs}$  levels have undergone small oscillations along the depth, maximum peaks of radionuclide deposition being observed at 18 cm deep (PA), 30 cm deep (PF) and 19 cm deep (CR-III). As expected the cores PF and CR-III showed low levels for the radionuclides, since the cores have a high sand concentration. The increase of the sand percentage in the sediments causes a diluting effect in the radionuclides absorption by the sediments.

Although the Cananeia-Iguape estuary did not had any test or nuclear accident reported, the presence of  $^{137}\text{Cs}$  sediment is due to the atmospheric fallout phenomenon, because of the world-wide distribution of the radionuclide from nuclear explosions by the atmospheric currents.<sup>17</sup>

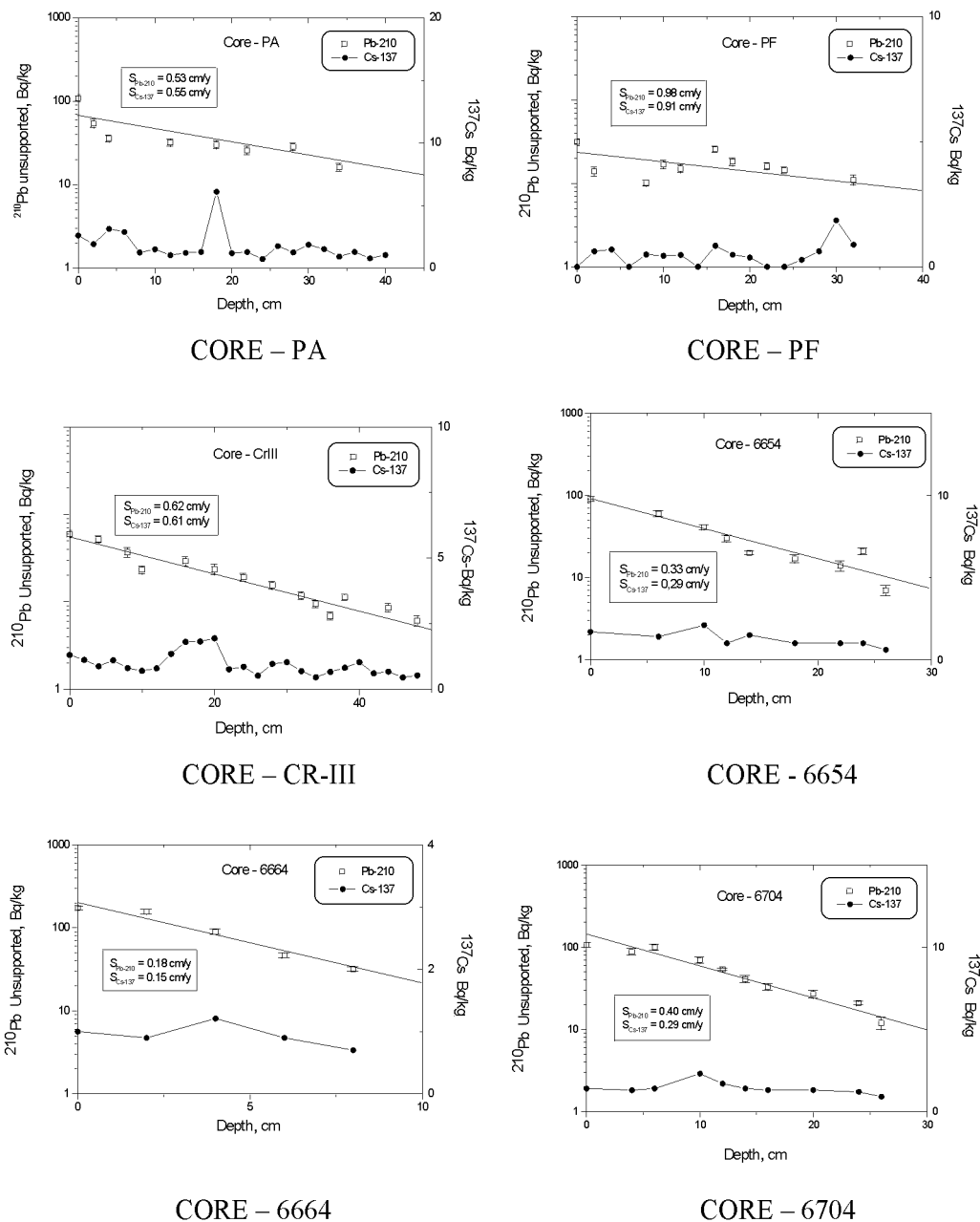


Fig. 4.  $^{210}\text{Pb}$  unsupported and  $^{137}\text{Cs}$  as a function of depth for cores and sedimentation rates in the Cananeia-Iguape estuary and in the southern continental shelf

The sedimentation rates obtained by  $^{210}\text{Pb}$  dating, in the sediment columns along the Cananeia-Iguape estuary were of  $0.53 \text{ cm}\cdot\text{y}^{-1}$  (PA),  $0.62 \text{ cm}\cdot\text{y}^{-1}$  (CR-III) and  $0.98 \text{ cm}\cdot\text{y}^{-1}$  (PF). The relative errors between the sedimentation rates for the cores analyzed by the two radionuclides ( $^{210}\text{Pb}$  and  $^{137}\text{Cs}$ ) ranged from 2 to 9%, showing a good agreement between the values. The simultaneous uses of these two radionuclides have given more accurate data.

During the ebb-tide, the matter not deposited in the canal is transferred preferably to deposit in the swamp areas in expansion, as observed in PF. The remaining internal canals, which do not receive the direct influence of Ribeira drainage, are directly affected by the Canal do Mar Pequeno ebb-tide, show sedimentation rates lower than the more external canals of this system (Mar de Cananeia and Mar Pequeno).

The determinations of natural and artificial radionuclides from the cores collected in the continental platform and slope indicated a continuous decay of the radionuclide values between the present bottom surface and the horizons closest to 30 cm depth.

The agreement obtained among the sedimentation rates for the radionuclides  $^{210}\text{Pb}$  and  $^{137}\text{Cs}$ , in the analyzed cores, showed rates ranging from 0.15 to  $0.40\text{ cm}\cdot\text{y}^{-1}$  for the south Sao Paulo platform and the slope. These values (although only indicating the size measurement of the superior Holocene sedimentation in the Brazilian south/south-eastern platform and consequently of the Brazilian continental mechanism of terrestrial sedimentation) in the south platform of Sao Paulo, are related to the dynamic of water masses, specially the stressed seasonal relocation of the Tropical Waters (TW) and the South Atlantic Central Waters (ACAS), which are responsible for the transfer and deposition of the muddy sedimentation in the coastal region, mainly by the drainage of the Ribeira de Iguape river.

\*

The authors would like to thank FAPESP, CNPq, CNEN and Oceanographic Institute (IO/USP) for the financial support.

### References

1. M. KOIDE, A. SOUTAR, E. D. GOLDBERG, *Earth Planet Sci. Letters*, 14 (1972) 442.
2. L. U. JOSHI, T. L. KU, *J. Radioanal. Nucl. Chem.*, 52 (1979) 329.
3. M. RAVICHANDRAN, M. BASKARAN, P. H. SANTSCHI, T. S. BIANCHI, *Chem. Geol.*, 125 (1995) 291.
4. J. D. EAKINS, IAEA-TECDOC-298, 1983, p. 31.
5. G. KIRCHENER, H. EHLERS, *J. Coastal Res.*, 14 (1998) 483.
6. Z. ZUO, D. EISMA, R. GIELES, J. BEKS, *Deep-Sea Res. II*, 44 (1997) 597.
7. C. C. FULLER, A. V. GENN, M. BASKARAN, R. ANIMA, *Mar. Chem.*, 64 (1999) 7.
8. B. L. K. SOMAYAJULU, R. BHUSHAN, A. SARKAR, G. S. BURR, A. J. T. JULL, *Sci. Total Environ.*, 237/238 (1999) 429.
9. B. M. CASTRO FILHO, L. B. MIRANDA, S. Y. MYAO, *Bolm. Inst. Oceanogr.*, 35 (1987) 135.
10. M. M. MAHIQUES, Associate Professorship Thesis, Oceanographic Institute of Sao Paulo University, 1998, p. 86.
11. EGG&Ortec, Maestro II Software Model A64-BI Operator Manual, USA, 1992.
12. I. I. L. CUNHA, R. C. L. FIGUEIRA, R. T. SAITO, *J. Radioanal. Nucl. Chem.*, 239 (1999) 477.
13. International Atomic Energy Agency, Catalogue of Reference Materials. IAEA, Vienna, 2000.
14. G. R. HELZ, G. H. SETLOCK, A. Y. CANTILLO, W. S. MOORE, *Earth Planet Sci. Letters*, 76 (1985/1986) 23.
15. P. McDONALD, G. T. COOK, M. S. BAXTER, *Proc. Intern. Symp. on Radionuclides in the Study of Marine Process*, Norwich, United Kingdom, Sept., 1991.
16. M. BASKARAN, S. NAIDU, *Geochim. Cosmochim. Acta*, 59 (1995) 4435.
17. R. C. L. FIGUEIRA, L. R. N. SILVA, A. M. G. FIGUEIREDO, I. I. L. CUNHA, *Proc. Intern. Conf. on the Radiological Accident of Goiania – 10 years later*, Goiania, Brazil, Oct., 1997.
18. I. OTHMAN, T. YASSINE, I. S. BHAT, *Sci. Total Environ.*, 153 (1994) 57.
19. G.-H. HONG, S.-H. LEE, S.-H. KIM, C.-S. CHUNG, M. BASKARAN, *Sci. Total Environ.*, 237/238 (1999) 225.
20. U. S. KUMAR, S. V. NAVADA, S. M. RAO, R. P. NACHIAPPAN, B. KUMAR, T. KRISHNAMOORTHY, S. K. JHA, V. K. SHUKLA, *Appl. Radiation Isotopes*, 51 (1999) 97.
21. C. A. HUH, H.-Y. CHEN, *Mar. Pollut. Bull.*, 38 (1999) 545.
22. C.-A. HUH, C.-C. SU, *Mar. Geol.*, 160 (1999) 183.